JOURNAL OF MATERIALS SCIENCE: MATERIALS IN MEDICINE 7 (1996) 167–174

Mechanical and histological evaluations of cobalt–chromium alloy and hydroxyapatite plasma-sprayed coatings in bone

C. Y. YANG*, B. C. WANG, W. J. CHANG, E. CHANG
Departments of Orthopaedics and Materials Science and Engineering, National Cheng Kung University, Tainan, Taiwan*

J. D. WU
Industrial Technology Research Institute, Hsinchu, Taiwan

This study evaluated the mechanical and histological behavior of cobalt–chromium (CoCr) alloy and hydroxyapatite (HA) plasma-sprayed coatings in canine cortical bone after 6 and 12 weeks of implantation, using CoCr alloy as the substrate. The substrate was bond-coated with microtextured CoCr alloy coating to ensure adherence between the substrate and top coats. A macrotextured CoCr alloy top coat with surface roughness $R_a = 34.25 \pm 5.50$ μm was produced to create suitable pores ranging from 25 μm to 200 μm for bone ingrowth. For HA top coat, a relatively smooth surface ($R_a = 15.14 \pm 3.21$ μm) was prepared for bone apposition. Shear testing of bone/implant interfaces showed that the CoCr alloy top coat exhibited significantly lower ($p < 0.01$) mean shear strength than the HA top coat at each time interval. The maximum shear strength was 10.88 ± 0.38 MPa for HA-coated implants 12 weeks post-implantation. After histological evaluations, substantial differences in the extent of new bone formation and the types of implant/bone contact were found between two kinds of implants. Direct bone-to-HA coating contact was consistently observed, while a layer of fibrous tissue intervening at the bone–CoCr alloy coating interface was found. Occasionally, partial dissolution of HA coating was seen after 12 weeks of implantation. The results of this study suggested that plasma-sprayed macrotextured CoCr coatings may not be an effective alternative for biological fixation.

1. Introduction

As long-term complications of cemented fixation become evident [1, 2], the concept of biological fixation either by bone ingrowth into porous metallic coatings or by bone apposition onto bioactive calcium-phosphate coatings has become increasing popular. Whether such implants will be successful has yet to be determined.

Regarding the ultimate performance of implants with porous sintered-bead coatings, however, several concerns or limitations have been raised. First, material characteristics of this implant system have changed adversely for implantation. These include the effects of increased metal ion release due to increased surface area [3, 4], the serious reduction in substrate fatigue strength owing to high temperature sintering [5, 6], and the potential loss or delamination of the porous coating [3, 7]. Second, a good tight fit during surgery is needed to ensure implant–bone apposition and minimize micromotion [8]. Third, restricted activity or even immobilization of the patients is necessary for bone tissue ingrowth to occur for the first 6 to 8 weeks after implantation [9], as there is no adherence of the porous surface to the bone at the time of surgery. Fourth, the highest obtainable shear strength at bone–implant interface is limited to 30–40% [10] of that of cortical bone since the surface pores available for tissue ingrowth are limited. The need for achieving better component stability is, thus, obvious.

In a study by Luckey *et al.* [11], the biological fixation capability of a nonporous, high-integrity plasma-sprayed CoCr (ASTM F75 alloy) coating was compared to a conventional sintered-bead CoCr coating in goats. The plasma-sprayed CoCr coating was developed to minimize the adverse changes in material characteristics compared to the sintered porous-beaded devices. Their results showed that the CoCr coating might offer potential advantages over conventional porous coatings and therefore seemed to be an effective alternative. More recently, the uses of plasma-sprayed hydroxyapatite (HA) coatings, in comparison with porous coating, were documented to reveal many advantages. These included the formation of chemical bonding at the HA/bone interface [10, 12], the promotion of normal bone formed along the HA layer [13–19], and the protection of surrounding bone against metal-ion release from a metal prosthesis [20]. Therefore, HA-coated metal

0957–4530

implants seem promising for application in orthopaedic surgery.

The adherence between coatings, especially ceramic, and the metal substrate is important in providing long-term fixation since mechanical failure occurring at the ceramic–metal substrate interface has consistently been reported [10, 21–23]. Calcium-phosphate coatings on metal substrates pretreated with porous sinter-beaded coating [24–29] or macrotextured grooves [30] have been shown to significantly enhance bone apposition and attachment strength at the bone–implant interface. Methods must be developed, therefore, to protect the relatively weak coating–substrate interface from direct shear loading.

In this study, the osseous and mechanical responses to two coatings, namely, plasma-sprayed macrotextured CoCr alloy coating and HA coating, were compared.

2. Materials and methods

2.1. Implant fabrication

Cylindrical rods (4.26 or 4.46 mm diameter × 12 mm length) of CoCrMo alloy, conforming to ASTM F75, were used as substrates (Fig. 1a). The substrate rods were precoated with microtextured CoCr alloy coating (approximately 100 μm) which served as bond coat by plasma spraying (Fig. 1b). Then, implants with two kinds of top coat were prepared for *in vivo* implantation (Fig. 1c): (1) a macrotextured plasma-sprayed CoCr (PSCO) alloy coating (approximately 150 μm) and (2) a plasma-sprayed HA (PSHA) coating (approximately 50 μm). Different initial substrate diameters were used to produce specimens with approximately the same finished diameter (4.76 ± 0.05 mm).

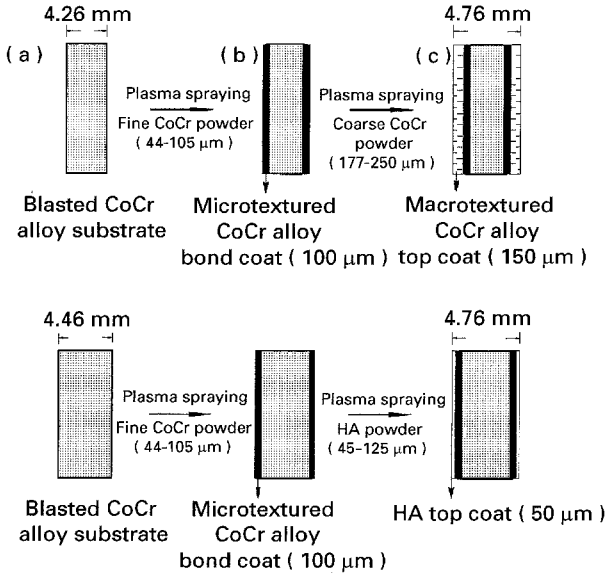

Figure 1 Schematic configuration of implant preparation: (a) cylindrical rods of CoCr alloy substrate with different initial diameter; (b) plasma-sprayed bond-coat of microtextured CoCr alloy coating (100 μm); and (c) plasma-sprayed macrotextured CoCr alloy top coat (150 μm) and HA top coat (50 μm). The finished implant diameter was 4.76 mm.

TABLE I The plasma spraying parameters used for preparing bond coat and top coats

Spraying parameters	Bond coat	Top coats	
		PSCO	PSHA
Primary gas, flow rate (l min^{-1})	Ar, 41	Ar, 41	Ar, 41
Secondary gas, flow rate (l min^{-1})	H_2, 6	H_2, 11	H_2, 6
Powder carrier gas, flow rate (l min^{-1})	Ar, 3	Ar, 5	Ar, 3.2
Powder feed rate (g min^{-1})	33	12	20
Powder (kW)	35	42	35
Stand-off distance (cm)	18	12	7.5
Surface speed (cm min^{-1})	240	240	240
Transverse speed (cm min^{-1})	60	60	60

Prior to spraying, the substrate surfaces were degreased to remove organic contaminants and blasted with Al_2O_3 grit to roughen the surface. All coatings used in this study were applied by means of an atomospheric plasma spray technique (APS, Plasma-Technik, M 1100-C). The plasma spraying parameters for preparing the bond coat and top coats are listed in Table I.

For creating the bond coat, fine spherical CoCr alloy powder (ASTM F75, 44–105 μm, Nuclear Metals, Inc.) was used in the coating process. This thin layer of bond coat was intended to ensure adherence between the substrate and the top coat. The surface morphology and the cross-sectional structure of the bond coat are shown in Fig. 2a and Fig. 3a, respectively. For preparing the PSCO top coat, coarse spherical CoCr alloy powder (ASTM F75, 177–250 μm, Nuclear Metals, Inc.) was used to obtain a macrotextured coating (Fig. 2b and Fig. 3b), which exhibited an R_a surface roughness of approximately 34.25 ± 5.50 μm. As shown in Fig. 3b, suitable pore size ranging from 25 μm to 200 μm (mostly 50–100 μm) was created for bone ingrowth. With regard to the PSHA top coat, a uniform thickness of about 50 μm was produced (Fig. 2c and Fig. 3c) using high purity HA powder (Amdry 6020, Sulzer Plasma Technik, Inc.). The surface roughness (R_a) for PSHA coating was about 15.14 ± 3.21 μm. X-ray diffraction analysis indicated that the PSHA coating consisted of about 40% of original crystalline structure and 90% apatite with 10% extra phases ($Ca_3(PO_4)_2$, CaO, and $Ca_4P_2O_9$) [32].

2.2. Surgical technique

All implants were cleaned with a 15-min ultrasonic wash in reagent grade acetone followed by a 15-min ultrasonic rinse in distilled water. Dry heat (120° C, 8 h) sterilization was used prior to implantation.

The lateral femoral cortices of adult, bone-matured mongrel dogs weighing 10–15 kg were drilled transcortically by three-stage reaming to the final diameter, using a sterile surgical technique. Dogs were anesthetized with 50 mg/kg of sodium thiopentone (Pentothal, Abbott, Australasia Pty. Ltd.). Cefazolin (i.v. 1 g) and gentamicin sulfate (i.m. 40 mg) were given

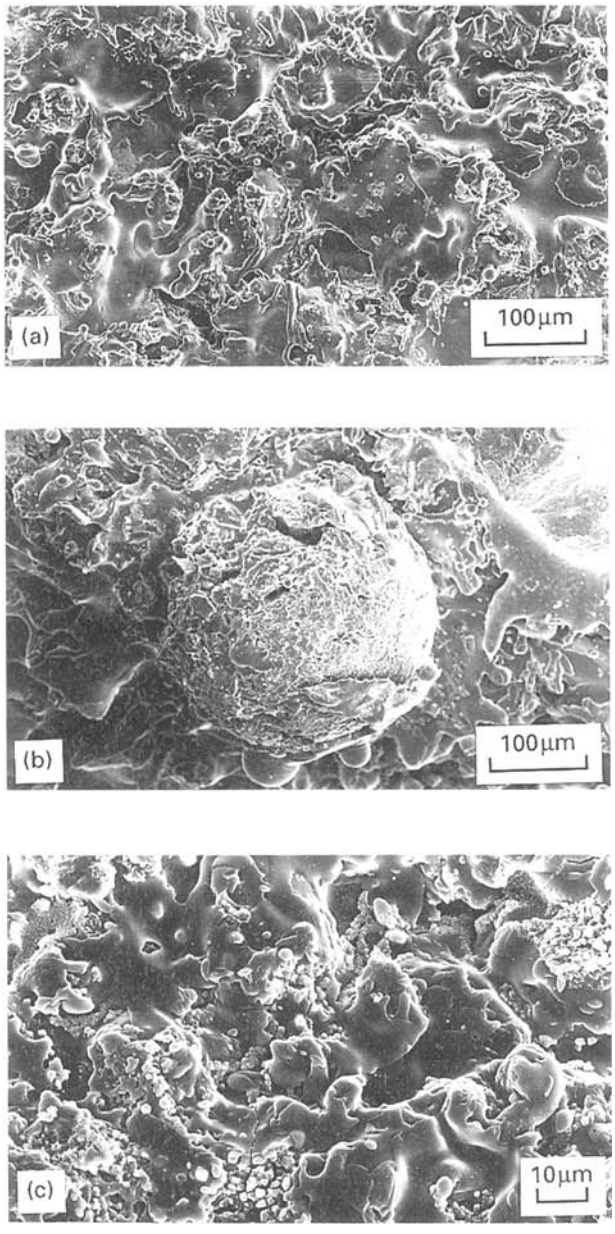

Figure 2 Surface morphology of: (a) microtextured CoCr alloy bond coat; (b) macrotextured PSCO top coat; and (c) the PSHA top coat.

during surgery as prophylactic antibiotics. During drilling procedures copious saline was used to minimize any bone thermal trauma and to remove the bone debris. The drill sequence employed 1.587 mm and 3.175 mm drill bits. Final sizing was done using a 4.76 mm drill to produce a hole almost equal to the diameter (4.76 mm) of the implants. Then, implants with PSCO and PSHA coatings were bilaterally inserted into pre-drilled holes by finger pressure. A total of 60 implants were inserted into the femora of six dogs. Each femur contained five implants; four implants for mechanical testing and one implant for histological evaluation.

2.3. Mechanical testing

Three dogs were sacrifice at each of 6 and 12 weeks postoperatively. The intact femora were retrieved and cleared of soft tissue. By using a diamond saw

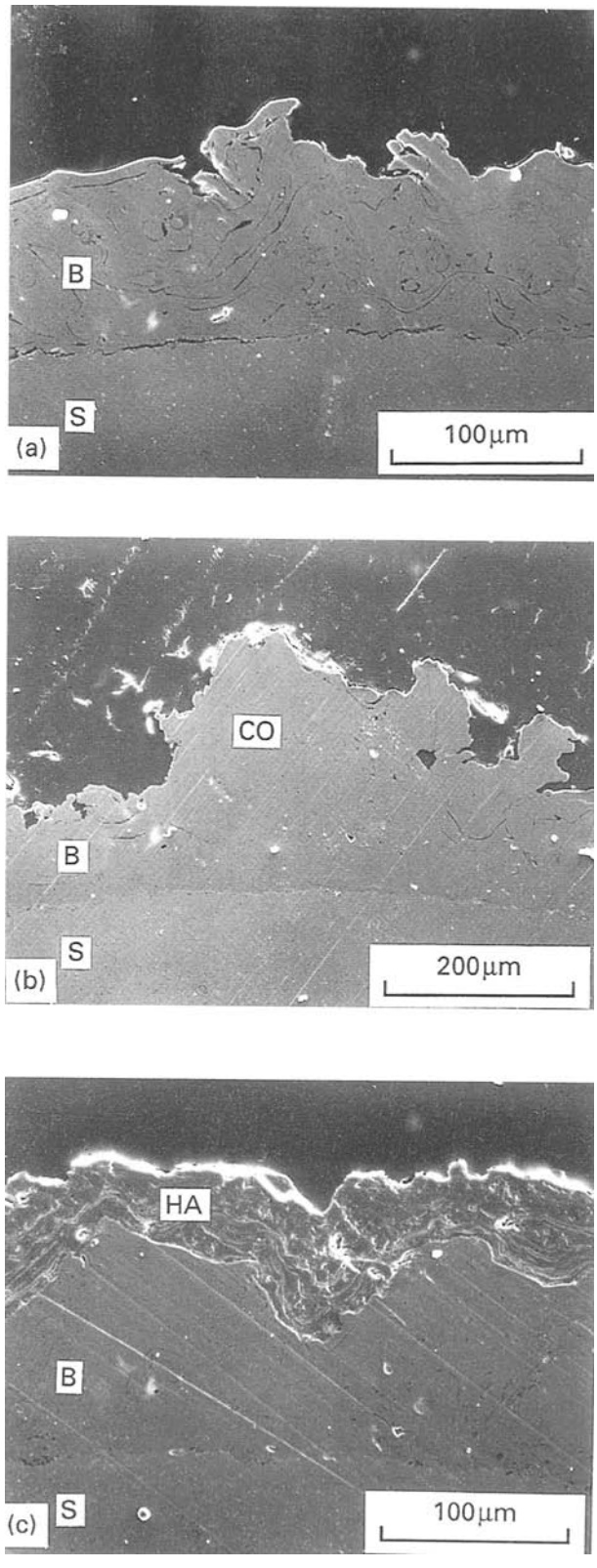

Figure 3 Cross-sectional structure of: (a) microtextured CoCr alloy bond coat; (b) macrotextured PSCO top coat; and (c) the PSHA top coat. B, bond coat; S, substrate; CO, PSCO top coat; HA, PSHA top coat.

(Isomet), each implant site was isolated transversely and then bisected through the medullary cavity perpendicularly to the long axis of implant. A trephine-type reamer made of 316 stainless steel was used to prepare a smooth endosteal bone surface surrounding each implant. Well-prepared, fresh samples were placed in a testing jig, and the implants were pushed

TABLE II Shear strength of the implant–bone interface (MPa)

Weeks	Shear strength (MPa)	
	PSCO implants	PSHA implants
6	1.85 ± 0.59 ($n = 12$)	10.30 ± 0.39[a] ($n = 12$)
12	1.27 ± 0.72 ($n = 12$)	10.88 ± 0.38[a] ($n = 12$)

Values are given as mean $\pm$ SD (standard deviation)
n: the number of samples tested.
[a] Significant difference ($p < 0.01$) between the PSCO and PSHA implant.

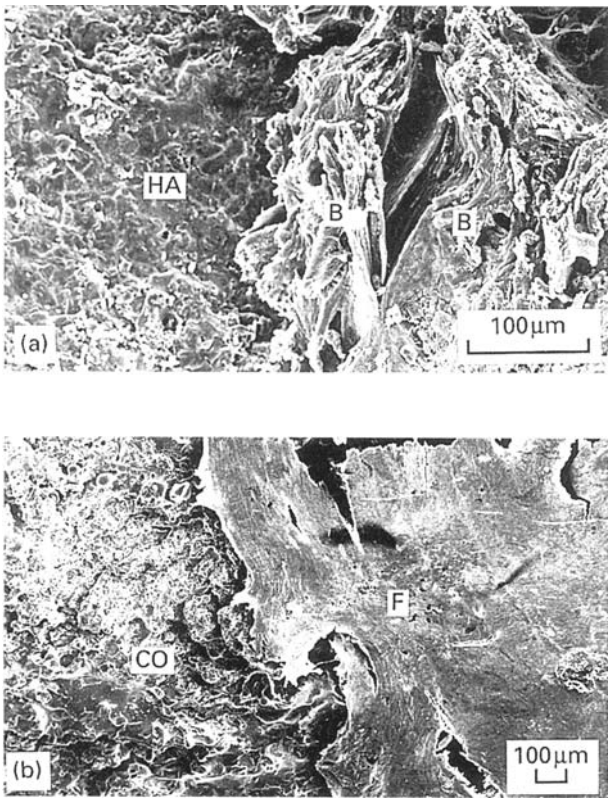

Figure 4 Fractographs of implants after the push-out test showing the failures were conclusively at: (a) the bone–PSHA coating interface and (b) the bone–PSCO coating interface 12 weeks postimplantation. HA, PSHA top coat; B, bone; CO, PSCO top coat; F, fibrous tissue.

out from the surrounding bone using an Instron test machine. A loading rate of 0.2 mm/min was used for all tests. The force needed to move the implant was determined from the load–displacement curve. The shear strength at the implant/bone interface was calculated by dividing the maximum push-out force by the total bone area in contact with the implant. This area was represented by the following formula:

$$\text{area} = \pi DH$$

where D is the diameter (4.76 mm) of the implant and H is the average cortex thickness. The cortex thickness was measured on both sides of the implant with a dial caliper micrometer, and the average of these two measurements was taken as the average cortex thickness. The experimental techniques used have been reported in a previous study [31]. Shear strength of PSCO-coated versus PSHA-coated implants were statistically compared by a paired t-test.

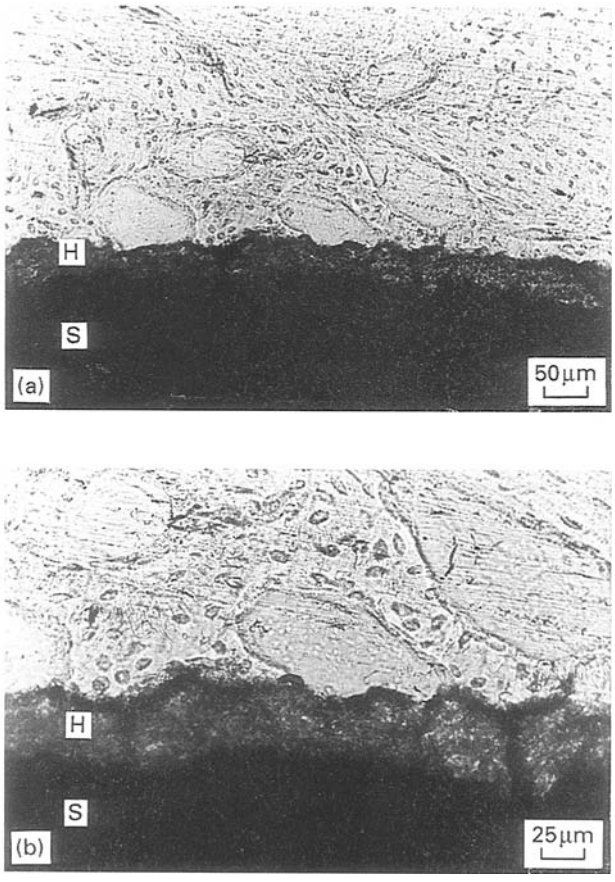

Figure 5 Histological appearance of the interface of cortical bone and PSHA implant 6 weeks postimplantation. Section revealed: (a) bone apposition to the PSHA coating and (b) a direct bone–PSHA coating contact. S, bond-coated substrate; H, PSHA top coat.

After the push-out test, the disrupted implants were fixed in 10% buffered formalin solution, dehydrated in graduated ethyl alcohol solutions from 70–100%, and then carbon coated. The fracture surfaces of implants were investigated by scanning electron microscope (SEM) for failure mode anlayses.

2.4. Histological evaluation

The implants which were not subjected to mechanical testing were fixed in 10% buffered formalin solution and dehydrated in graduated ethyl alcohol solutions from 70–100%. They were then embedded in polymethylmethacrylate (PMMA). Each undecalcified implant block was sectioned perpendicularly to the long axis of the implant into two to three thin slices (300–400 μm) in the cortical bone region. The slice was polished flat with fine sanding strips and mounted on a glass slide with a fast drying glue. After drying, the slice was hand ground to approximately 30–40 μm, polished by diamond paste (6 μm), and viewed unstained by transmission light microscope.

3. Results

The surgical operation was tolerated well by the dogs. There were no complications noted during the periods. At harvesting, there were no signs of infection or

metallic staining around the implants, which were firmly fixed to the surrounding bone.

3.1. Mechanical testing

The interface shear strength data of implants obtained from the push-out tests are summarized in Table II. A paired t-test was used to determine significant differences (defined as $p < 0.01$) among the values.

It is clear from Table II that the PSHA implants displayed significantly higher mean shear strength than the PSCO implants at each time period. After 6 weeks of implantation, shear strength of 10.30 ± 0.39 MPa was observed in the PSHA implants, implying that the PSHA implant had a dominant effect on initial fixation. After evaluating the localization of the disruption of the PSHA implants, it was found that the specimens failed conclusively at the bone/HA coating interface (Fig. 4a). Since the PSCO implant could be dislodged easily during mechanical testing, low shear strengths ranging from 1 to 3 MPa were measured at 6 and 12 weeks, indicating that these implants could not offer biological stability to bone. With fibrous tissue covered on the microtextured PSCO coating, the failure site was in all cases at the bone/PSCO coating interface (Fig. 4b).

3.2. Histology

Substantial variations in the extent of new bone formation and the types of bone/implant contact were found between the PSCO and PSHA implants. These variations appeared to result from different biological responses to the surface layer of the implants.

At 6 weeks, new bone was intimately apposed to the PSHA coating (Fig. 5a). Along the PSHA coating, a direct bone-to-HA coating contact (osseointegration) was observed (Fig. 5b). On the contrary, in the PSCO implant, only part of the space between the pre-existing bone and the PSCO coating was filled with new bone as shown in Fig. 6a. A thick layer of fibrous tissue intervening at the bone/PSCO coating interface was evident (Fig. 6b).

After 12 weeks of implantation, bone proliferation was found at the bone/PSHA coating interface (Fig. 7a), compared to that shown in Fig. 5a. The phenomenon of osseointegration was still apparent (Fig. 7b). On the other hand, bone ingrowth into the PSCO coating has been found in some regions (arrow in Fig. 8a). However, a relatively thin layer of fibrous tissue still interposed at the bone/PSCO coating interface (Fig. 8b), suggesting that the PSCO coating does not conform to the concept of osseointegration. It is worth noting that signs of partial dissolution of PSHA coating were observed occasionally at bone/PSHA coating interface as indicated by the arrow in Fig. 9a

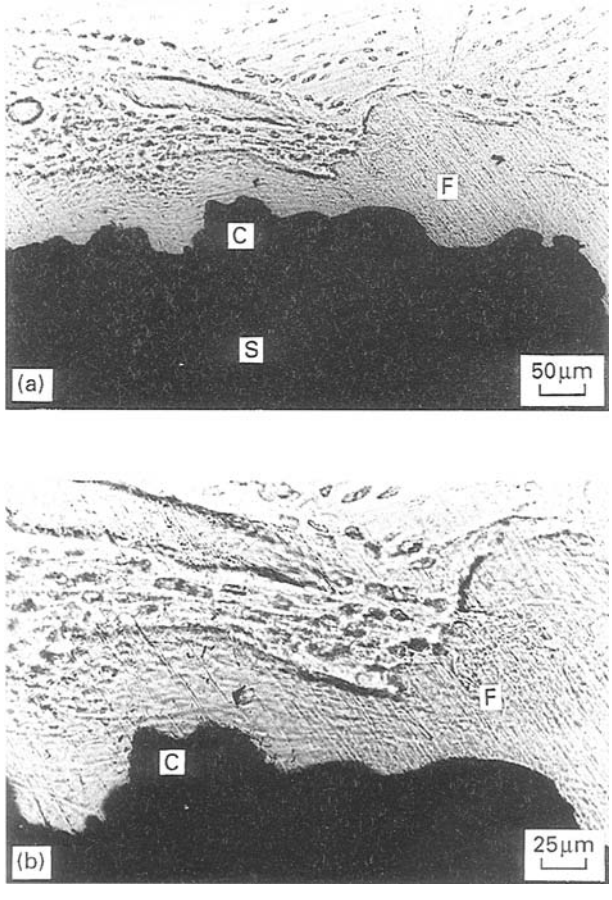

Figure 6 Histological appearance of the interface of cortical bone and PSCO implant 6 weeks postimplantation. Section revealed: (a) only part of the new bone has filled the space between the pre-existing bone and the PSCO implant and (b) a thick layer of fibrous tissue intervening at the bone-PSCO coating interface. S, bond-coated substrate; C, the PSCO top coat; F, fibrous tissue.

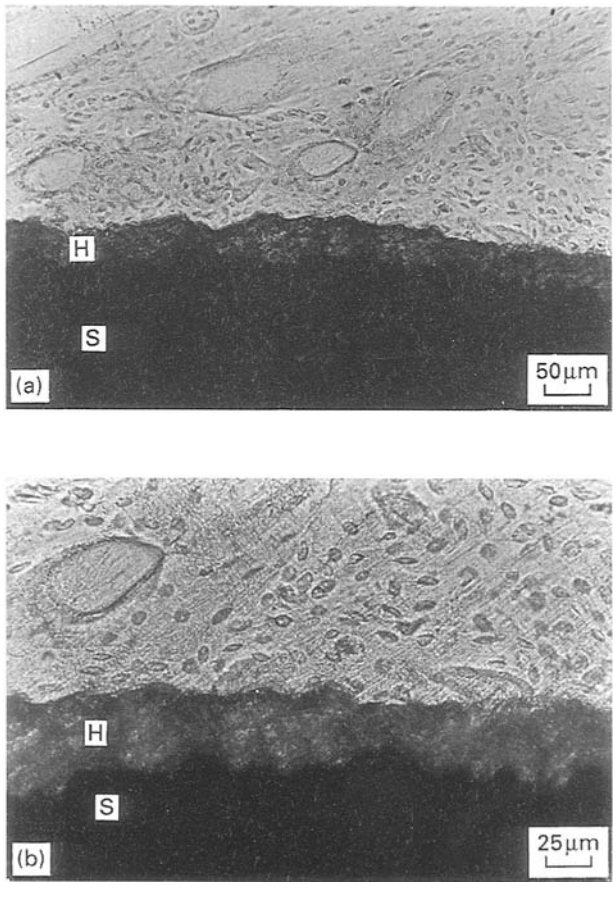

Figure 7 PSHA implant–cortical bone interface 12 weeks postimplantation: (a) bone proliferation was found and (b) a direct bone–PSHA coating contact still presented. S, bond-coated substrate; H, the PSHA top coat.

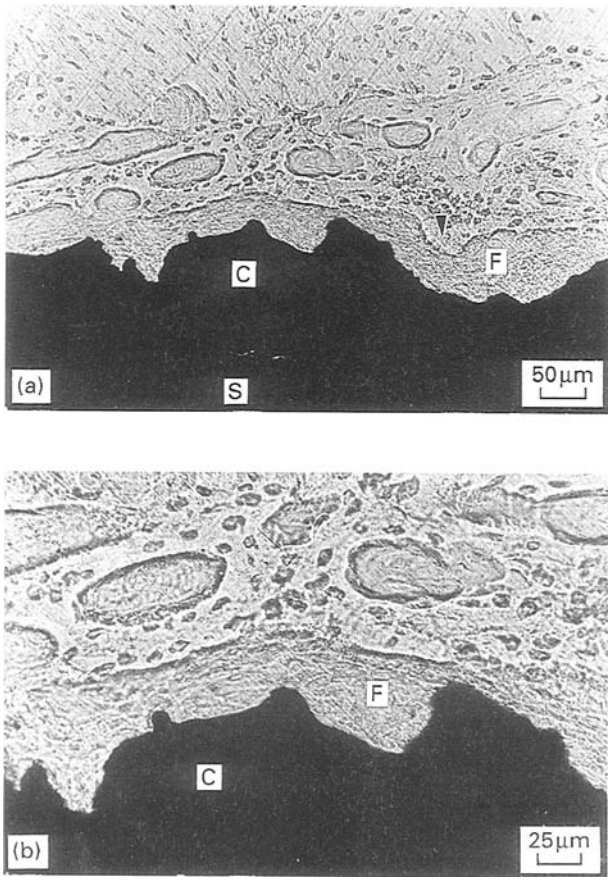

Figure 8 PSCO implant–cortical bone interface 12 weeks postimplantation: (a) bone ingrowth into the PSCO coating was found and (b) a relatively thin layer of fibrous tissue interposing at the bone–PSCO coating interface still presented. S, bond-coated substrate; C, the PSCO top coat; F, fibrous tissue.

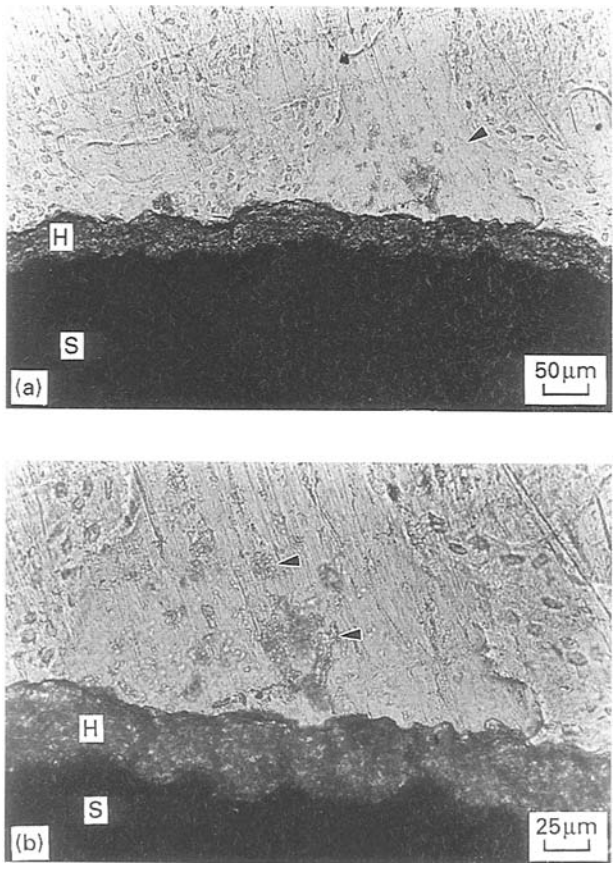

Figure 9 (a) Partial dissolution of HA coating observed in the remodelling canals at the bone–HA coating interface as indicated by arrow 12 weeks postimplantation. (b) Higher magnification of arrow in (a). S, bond-coated substrate; H, the PSHA top coat.

12 weeks postimplantation. Within the remodelling canals, granular particles dissociated from the PSHA coating were seen (Fig. 9b). This finding was similar to the results of our previous study [18].

4. Discussion

In a previous study [31], the effect of coating thickness on the shear strength of plasma-sprayed HA coatings was investigated. In achieving reliable implant-to-bone fixation, 50 μm HA coating on Ti–6Al–4V alloy substrate was shown to be a successful implant system. In this study, we investigated further two kinds of implant systems, namely, PSCO coating and PSHA coating on CoCr alloy substrate, which was bond-coated with microtextured CoCr alloy coating to ensure strong adherence between the top coats and the substrate.

The shear strengths of plasma-sprayed calcium-phosphate coatings on porous-coated implants yielded variable results (Table III). Cook *et al.* [25], in a study of plasma-sprayed HA coating on sintered porous CP titanium implant in dogs, found that shear strength after 6 and 12 weeks was 14.19 and 17.92 MPa, respectively. These strength values revealed no statistically significant difference compared to the uncoated specimens. In later research by the same group [28], the shear strength of sintered porous CoCrMo coating with and without plasma-sprayed HA coating was evaluated in a transcortical implant model in dogs. The results demonstrated enhanced attachment strength in HA-coated samples (12.80 MPa at 6 weeks and 15.73 MPa at 12 weeks) compared to the uncoated ones at all time periods. In the tibia of mature goats, the shear strength of porous Ti–6A1–4V beads with or without plasma-sprayed HA coating was assessed by Oonishi *et al.* [24]. Their results showed that the HA-coated implants exhibited significantly higher strength (13.87 MPa) than the controls (7.35 MPa) at 6 weeks, while no differences existed for two implants (around 24.92 MPa) at 12 weeks. Rivero and coworkers [27] studied plasma-sprayed calcium-phosphate (mostly tricalcium phosphate, TCP) coatings applied to titanium fibre mesh porous intramedullary implants in dogs. Significantly greater attachment strength was reported for the TCP-coated implants (2.75 MPa) after 4 weeks of implantation compared to the uncoated controls (2.22 MPa). In a study by Chae *et al.* [29], TCP-coated porous CoCrMo intramedullary implant rods were prepared in rabbits. Similar pull-out force was reported between TCP-coated (307 N) and uncoated specimens (324.7 N) at 12 weeks. The findings of these studies indicated that HA coatings applied to porous metal substrate could improve implant–bone attachment strength.

TABLE III Mean shear strength (MPa) of plasma-sprayed calcium-phosphate coatings on porous-coated substrate obtained in various studies

Weeks	Cook [25]	Cook [28]	Mean shear strength		Chae [29]	Yang (this study)	
			Oonishi [24]	Rivero [27]			
1				0.75 ± 0.09			
2		5.04 ± 1.79	1.32	2.72 ± 0.23			
3	7.52 ± 2.44						
4		9.17 ± 4.20	4.34	2.75 ± 0.24			
6	14.19 ± 3.99	12.80 ± 2.30	13.87	2.61 ± 0.19		10.30 ± 0.39	1.85 ± 0.59
8		12.60 ± 2.72					
12	17.92 ± 5.46	15.73 ± 2.36	24.92		324.7 N*	10.88 ± 0.38	1.27 ± 0.72
18		23.15 ± 3.64					
26		27.06 ± 2.36					
52		21.21 ± 3.80					
Top coat	PS–HA	PS–HA	PS–HA	PS–CAP	PS–TCP	PS–HA	PSCO
Bond coat	CP Ti Beads	CoCrMo Beads	Ti–6Al–4V Beads	CP Ti fibers	CoCrMo Beads	PS–CoCrMo	PS–CoCrMo
Substrate	Ti–6Al–4V	CoCrMo	Ti–6Al–4V	Ti–6Al–4V	CoCrMo	CoCrMo	CoCrMo
Implant mode	Transcortical	Transcortical	Transcortical	Intramedullary	Intramedullary	Transcortical	Transcortical
Animal	Dogs	Dogs	Goats	Dogs	Rabbits	Dogs	Dogs

N* denotes newton, otherwise values are given as mean ± SD (standard deviation).
PS, plasma-sprayed; HA, hydroxyapatite; CAP, calcium-phosphate; TCP, tricalcium-phosphate; CO, CoCrMo alloy.

For our experiments, the measured shear strength (around 10 MPa) appeared to be a little lower than that found by Cook and coworkers [25, 28]. The variation might be attributed to differences in the porous layers (materials, surface roughness and pore size) and the HA coating (degree of crystallinity, impurity phases, Ca/P ratio, bonding strength, and surface roughness). More recently, Dhert *et al.* [33] further pointed out that clearance of the hole in the support jig, Young's modulus of the implant, cortical thickness, and implant diameter might influence the results of shear strength measurements.

With regard to the macrotextured PSCO coatings in this present study, a very low shear strenth (around 1–3 MPa) was obtained. This finding was markedly inconsistent with that of Luckey *et al.* [11], who investigated the shear strength of plasma-sprayed CoCr alloy coating and conventional sintered bead coating in cortical and cancellous bone of dogs after 8 and 16 weeks of implantation. Their results revealed that although the plasma-sprayed CoCr alloy coating exhibited lower overall average shear strength in cortical bone sites at both time periods (4.31 MPa at 8 weeks and 9.77 MPa at 16 weeks), the differences were not statistically significant. The surface roughness of CoCr alloy coating, the extent of press-fit, and the histological findings could be reasons why our results differed from theirs. Since higher surface roughness (RMS = 25 μm) of CoCr coating combining a uniform 2% press fit was used in their study, an area of the direct bone–CoCr coating contact was observed, resulting in shear strength equal to that of sintered bead coating. In this report, however, a lower surface roughness (R_a = 34.25 μm) of PSCO coating was evaluated. With non-interference fit, it is not surprising that there were no areas showing direct bone–PSCO coating contact (Figs 6 and 8), leading to lower shear strength. Nevertheless, further research is needed to confirm our findings.

As shown in Figs 5 and 7, the evidence of direct bone–PSHA coating contact was observed, being consistent with studies where osseointegration of HA coating was reported [13–19]. This led to the provision of strong implant-to-bone fixation. More attention should be paid to the signs of dissolution of the HA coating which were apparently noted 12 weeks postimplantation. This finding is similar to those of Denissen *et al.* [13] and Gottlander *et al.* [17] in which the pieces of HA loosened from the HA coating were observed within the remodelling canals at optical microscope level 1 year and 9 months postoperatively. In our previous report [18], the same phenomenon was demonstrated at the scanning electron microscope level. However, our finding cannot be further deduced to cell-mediated resorption as suggested by Manley [34]. In some cases, osteoclastic resorption of HA coating has been pronounced [15, 23, 35]. The biodegradation of HA coating suggested by our previous findings [31] and the dissolution of HA coating at 12 weeks might account for the same level of shear strength compared to that at 6 weeks.

The use of a thin layer of microtextured bond coat underlying the HA coating is considered important because it can ensure the adherence between the metal substrate and the HA coating. With failure occurring consistently at the bone–HA coating interface (Fig. 4a), the successful performance of the bond coat is, thus, noteworthy. A plasma-sprayed CP titanium bond coat applied between HA coating and Ti–6A1–4V substrate was performed in our laboratory [36]. Using the same transcortical mode in dogs, this implant obtained shear strength as high as 16.67 MPa at 12 weeks. The failure mode was in all cases at the bone–implant interface.

In this short-term study, the PSHA-coated CoCr alloy implant system was demonstrated to obtain strong fixation to bone, while the macrotextured PSCO-coated CoCr alloy implant system did not

provide suitable fixation to bone. A long-term study is needed to confirm our findings.

5. Conclusions

The biological fixation properties of two implant systems, namely, PSHA and macrotextured PSCO coating on CoCr alloy substrate precoated with microtextured CoCr bond coat, were assessed in the femoral cortices of canine after 6 and 12 weeks of implantation. The following concluding remarks may be made.

1. The PSHA implant displayed significantly higher shear strength than the PSCO implants at each time period studied. At 6 weeks, a shear strength of 10.30 ± 0.39 MPa could be obtained in the PSHA implants.

2. Across the HA coating, a direct bone-PSHA coating contact was evident, while a layer of fibrous tissue intervening at the bone–PSCO coating was observed.

3. The sign of partial dissolution of HA coating was seen after 12 weeks of implantation, and this was deduced not to be cell-mediated resorption.

4. With the very low shear strength (around 1–3 MPa) obtained, the macrotextured PSCO-coated CoCr alloy implant system may not offer an effective alternative for biological fixation. However, further study is needed to confirm our proposition.

Acknowledgements

The authors would like to thank Mr T. M. Lee for assistance in sample preparation. This study was done in cooperation with the Industrial Technology Institute, Hsinchu, Taiwan.

References

1. S. GOLDRING, A. SCHILLER, M. ROELKE, C. ROURKE, D. O'NEILL and W. HARRIS, *J. Bone Joint Surg.* **65-A** (1983) 575.
2. C. M. SUTHERLAND, A. H. WILDE, L. S. BORDEN and K. E. MARKS, *ibid.* **64-A** (1982) 970.
3. P. K. BUCHERT, B. K. VAUGHN, T. H. MALLORY, C. A. ENGH and J. D. BOBYN, *ibid.* **68-A** (1986) 606.
4. R. M. PILLIAR, *Clin. Orthop.* **176** (1983) 42.
5. T. KILNER, R. M. PILLIAR, G. C. WEATHERLY and C. ALLIBERT, *J. Biomed. Mater. Res.* **16** (1982) 63.
6. D. H. KOHN and P. DUCHEYNE, *ibid.* **24** (1990) 1483.
7. R. ROSENQUIST, B. BYLANDER, K. KNUTSON, U. RYDHOLM, B. ROOSER, N. EGUND and L. LIDGREN, *J. Bone Joint Surg.* **68-A** (1986) 538.
8. R. M. PILLIAR, J. M. LEE and C. MANIATOPOULOS, *Clin. Orthop.* **208** (1986) 108.
9. H. CAMERON, R. PILLIAR and I. McNAB, *J. Biomed. Mater. Res.* **10** (1976) 295.
10. R. G. T. GEESINK, K. de GROOT and P. A. K. T. CHRISTEL, *Clin. Orthop.* **225** (1987) 147.
11. H. A. LUCKEY, E. G. LAMPRECHT and M. J. WALT, *J. Biomed. Mater. Res.* **26** (1992) 557.
12. R. G. T. GEESINK, K. de GROOT and C. P. A. T. KLEIN, *J. Bone Joint Surg.* **70-B** (1988) 17.
13. H. W. DENISSEN, W. KALK, H. M. de NIEUPORT, J. C. MALTHA and A. van de HOOFF, *Int. J. Prosth.* **3** (1990) 53.
14. K. HAYASHI, K. UENOYAMA, N. MATSUGUCHI and Y. SUGIOKA, *J. Biomed. Mater. Res.* **25** (1991) 515.
15. D. BUSER, R. K. SCHENK, S. STEINEMANN, J. P. FIORELLINI, C. H. FOX and H. STICH, *ibid.* **25** (1991) 889.
16. J. A. JANSEN, J. P. C. M. van de WAERDEN, J. G. C. WOLKE and K. de GROOT, *ibid.* **25** (1991) 973.
17. M. GOTTLANDER and T. ALBREKTSSON, *Int. J. Oral Maxillofac. Imp.* **6** (1991) 339.
18. B. C. WANG, E. CHANG, C. Y. YANG and D. TU, *J. Mater. Sci. Mater. Med.* **4** (1993) 394.
19. B. C. WANG, E. CHANG, C. Y. YANG, D. TU and C. H. TSAI, *Surf. Coat. Tech.* **58** (1993) 107.
20. P. DUCHEYNE and K. E. HEALTH, *J. Biomed. Mater. Res.* **22** (1988) 1137.
21. S. D. COOK, K. A. THOMAS, J. F. KAY and M. JARCHO, *Clin. Orthop.* **232** (1988) 225.
22. C. P. A. T. CLEIN, P. PATKA, H. B. M. van der LUBBE, J. G. C. WOLKE and K. de GROOT, *J. Biomed. Mater. Res.* **25** (1991) 53.
23. W. J. A. DHERT, C. P. A. T. CLEIN, J. G. C. WOLKE, E. A. van der VELDE and K. de GROOT, *ibid.* **25** (1991) 1183.
24. H. OONISHI, M. YAMAMOTO, H. ISHIMARU, E. TSUJI, S. KUSHITANI, M. AONO and Y. UKON, *J. Bone Joint Surg.* **71-B** (1989) 213.
25. S. D. COOK, K. A. THOMAS, J. F. KAY and M. JARCHO, *Clin. Orthop.* **230** (1988) 303.
26. P. DUCHEYNE, J. BEIGHT, J. CUCKLER, B. EVANS and S. RADIN, *Biomaterials* **11** (1990) 531.
27. D. RIVERO, J. FOX, A. SKIPOR, R. URBAN and J. GALANTE, *J. Biomed. Mater. Res.* **22** (1988) 191.
28. S. D. COOK, K. A. THOMAS, J. E. DALTON, T. K. VOLKMAN, T. S. WHITECLOUD III and J. F. KAY, *ibid.* **26** (1992) 989.
29. J. C. CHAE, J. P. COLLIER, M. B. MAYOR, V. A. SUPRENANT and L. A. DAUPHINAIS, *ibid.* **26** (1992) 93.
30. K. A. THOMAS, J. F. KAY, S. D. COOK and M. JARCHO, *ibid.* **21** (1987) 1395.
31. B. C. WANG, T. M. LEE, E. CHANG and C. Y. YANG, *ibid.* **27** (1993) 1315.
32. C. Y. YANG, B. C. WANG, E. CHANG and J. D. WU, *J. Mater. Sci. Mater. Med.* **6** (1995) 249.
33. W. J. A. DHERT, C. C. P. M. VERHEYEN, L. H. BRAAK, J. R. de WIJN, C. P. A. T. KLEIN, K. de GROOT and P. M. ROZING, *J. Biomed. Mater. Res.* **26** (1992) 119.
34. M. T. MANLEY, in "Hydroxyapatite coatings in orthopaedic surgery", edited by R. G. T. Geesink and M. T. Manley (Raven Press, New York, 1993) p. 1.
35. T. W. BAUER, R. G. T. GEESINK, R. ZIMMERMAN and J. T. McMOHAN, *J. Bone Joint Surg.* **73-A** (1991) 1439.
36. T. M. LEE, B. C. WANG, E. CHANG and C. Y. YANG, unpublished work.

Received 1 June 1994
and accepted 19 June 1995